Journal of Nuclear Materials 434 (2013) 411–416

Contents lists available at SciVerse ScienceDirect

Journal of Nuclear Materials

journal homepage: www.elsevier.com/locate/jnucmat

Effect of lead factors on the embrittlement of RPV SA-508 cl 3 steel

Rodolfo Kempf [a,*], Horacio Troiani [b], Ana Maria Fortis [c]

[a] CNEA, Unidad Actividad Combustibles Nucleares, División Caracterización, Avda. Gral Paz 1499, C.P.B1650KNA, San Martín, Buenos Aires, Argentina
[b] Centro Atómico Bariloche (CNEA) e Instituto Balseiro (UNCU), CONICET, Av. Bustillo 9500, CP 8400, Rio Negro, Argentina
[c] CNEA, Departamento Estructura y Comportamiento, UNSAM, Avda. Gral Paz 1499, C.P.B1650KNA, San Martín, Buenos Aires, Argentina

ARTICLE INFO

Article history:
Received 12 September 2012
Accepted 5 December 2012
Available online 14 December 2012

ABSTRACT

This paper presents a project to study the effect of lead factors on the mechanical behaviour of the SA-508 type 3 Reactor Pressure Vessel (RPV) steel used in the reactor under construction Atucha II in Argentina. Charpy-V notch specimens of this steel were irradiated at the RA1 experimental reactor at a temperature of 275 °C with two lead factors (186 and 93). The neutron flux was 3.71×10^{15} n m^{-2} s^{-1} and 1.85×10^{15} n m^{-2} s^{-1} ($E > 1$ MeV) respectively. In both cases, the fluence was 6.6×10^{21} n m^{-2}, which is equivalent to that received by the PHWR Atucha II RPV in 10 years of full power irradiation. The results of Charpy tests revealed significant embrittlement both in the $\Delta T = 14$ °C and $\Delta T = 21$ °C shifts of the ductile–brittle transition temperatures (DBTT) and in the reduction of the maximum energy absorbed. This result shows that the shift of the DBTT with a lead factor of 93 is larger than that obtained with a lead factor of 186. Then, the results of irradiation in experimental reactors (MTR) with high lead factors may not be conservative with respect to the actual RPV embrittlement.

1. Introduction

In service, the exposure to energetic particles degrades the fracture toughness of the reactor pressure vessel (RPV) steels [1]. Ferritic steels change from ductile to brittle fracture when their deformation temperature falls below a critical value (the ductile-to-brittle transition temperature, DBTT). Irradiation embrittlement is typically characterized by an increase in the DBTT, marking the transition between the low toughness cleavage and high toughness ductile fracture regimes. Neutron irradiation increases the yield stress and decreases ductility. Irradiation hardening shifts the DBTT to higher temperatures by an amount (ΔT) that depends on the neutron dose and other factors such as the irradiation temperature and the steel composition. This shift may adversely affect the response of structural components when they are stressed in service or under transient conditions like a loss-of-coolant accident (LOCA).

The numerous works of characterization of RPV steels and specially prepared alloys [2–4] have revealed precipitation or agglomeration increased by radiation, mainly of Cu, Ni and Mn [5]. According to this, the most recent models of RPV embrittlement [6] include a component of hardening by dispersion based on the model of ageing developed by Russell and Brown [7], modified to take into account the diffusion increase caused by the over-saturation of vacancies as a result of radiation.

For a low intensity of fast flux ($E > 1$ MeV), the dose to achieve the contribution of the hardening peak by cooper rich precipitates (CRPs) is a function of the dose rate. This is more important at the low intensity of the typical flux of the Boiling Water Reactor (BWR) than for a pressurized water reactor (PWR) [8], thus highlighting the importance for the inside wall of the pressure vessel (RPV) of the Pressurized Heavy Water Reactor (PHWR) as Atucha II. The application of the ageing models developed by Russell and Brown [7] to the hardening and embrittlement was proposed for the first time by Fisher et al. [9,10].

Later, in 1998, improved embrittlement correlations of an advanced version of the archival Power Reactor Embrittlement database (PR-EDB) [11] were prepared by Eason, Wright and Odette for the U.S. Nuclear Regulatory Commission [12]. The importance of this report is that it explicitly introduces the mechanistic understanding of embrittlement in the analysis methodology of light water reactor RPV surveillance data. There is a general consensus that neutron irradiation induces microstructural change at the micro/nanometre level, being the main source of the mechanical degradation of steels [1–13]. The nanofeatures developed during the irradiation can be associated with two dominant forms of degradation, namely stable matrix defects (SMD), and copper- and manganese–nickel-rich precipitates (CRPs and MNPs), which are major sources of steel embrittlement through the hardening they produce [14–16].

Stable matrix damage (SMD) is due to the formation of agglomerates of point defects and dislocation loops during the irradiation. SMD is the dominant damage process for low-Cu steels, and the resulting dispersed barrier irradiation hardening scales roughly

* Corresponding author.
E-mail addresses: kempf@cnea.gov.ar (R. Kempf), troiani@cab.cnea.gov.ar (H. Troiani), fortis@cnea.gov.ar (A.M. Fortis).

0022-3115/$ - see front matter © 2012 Elsevier B.V. All rights reserved.
http://dx.doi.org/10.1016/j.jnucmat.2012.12.004

with the square root of fast fluence, and decreases with increasing irradiation temperature [14]. This behaviour is consistent with experimental mechanical property data and has also been modelled with success using atomistic simulations [3–18]. Experimental data indicate that SMD is independent of the dose rate over a range of five orders of magnitude in the dose rate [16].

CRP damage is linked to irradiation-enhanced formation of Cu-enriched solute clusters. Copper-rich clusters or precipitates are formed as a residue of annealing of vacancy-copper complexes or by normal nucleation because of the high copper super saturations. The contribution of CRP damage to the total DBTT depends on the Cu and Ni content of the steel and on the strong Cu–Ni interaction [5]. The CRP damage is a diffusion process where the time, together with the rate of point-defect production, plays an important role.

CRP damage is one of the two contributions to embrittlement better known experimentally. Both transmission electron microscopy (TEM) and techniques such as positron annihilation spectroscopy (PAS), Mössbauer spectroscopy (MS), thermoelectric power (TEP), anomalous small-angle X-ray scattering (ASAXS) [23] and small-angle neutron scattering (SANS) [22] have allowed the experimental characterization of the size of the precipitates, the relative number of these nanostructures, their composition and their volumetric fraction [19–21].

The dose rate effects on embrittlement are not yet fully understood [16]. Recently, there have been several studies on the neutron flux effect on irradiation hardening of RPV materials with different composition which put in discussion the dose rate effect [17]. These works explore multiple steels for RPV under different temperatures and subjected to neutron irradiation in different reactors with significantly different neutron spectra. In the present work, the neutron irradiations are carried out in the same reactor, varying only the flux intensity, i.e., keeping the neutron spectrum and irradiation temperature unchanged.

According to the present state of knowledge, the dose rate effects depend on the dose rate (fast flux) level, where the fast flux is defined as neutrons with $E > 1$ MeV. Three regions are identified [6–10]: low, intermediate, and high fast flux level. The dose rate effects are expected to occur over a wide range of flux of: (a) thermal contribution to Cu–Mn–Ni diffusion at low flux, (b) solute trap enhanced recombination over the intermediate range and (c) unstable matrix defect (UMD) sinks at the highest flux.

Both SMD and CRP damage involve an increase in the number of obstacles for the dislocation movement which causes the hardening and, consequently, the embrittlement of the steel. In a Charpy impact test, it is possible to consider that the DBTT obtained consists of two components:

$$\mathrm{DBTT} = \mathrm{DBTT}_{\mathrm{SMD}} + \mathrm{DBTT}_{\mathrm{CRP}}$$

In this project, it is intended to show that, under strict irradiation conditions (similar temperature and similar neutron spectrum), two lead factors give different results as a consequence of the differences in the structure of the radiation damage that occurs in different irradiation times.

2. Experimental

The CNEA-RA1 is a modified Argonaut-type light-water-moderated reactor, used for basic research. An irradiation facility was built and placed in the core of the RA1 reactor in order to obtain conditions similar to those of the materials of the RPV in a power reactor. The facility is an aluminium tube, the lower end of which is placed in the reactor core. Inside the tube, a low inertia electric furnace is placed in the position of maximum neutron flux and a capsule with eight Charpy V-notch specimens is placed inside the furnace. The tube is filled with inert gas and the gaps between the tube, the furnace and the capsule were calculated to obtain the best possible thermal transference. Temperature control is achieved through three thermocouples placed at different heights in the furnace as indicators of the temperature profile, and two thermocouples in the specimens, so that the temperature difference between them does not exceed 1 °C.

Table 1
Neutron spectrum.

Neutron energy (MeV)	Neutron flux (n m^{-2} s^{-1})
0–0.1	2.25×10^{16}
0.1–1	3.318×10^{15}
1–17.33	3.715×10^{15}

All irradiations were carried out in the same place of the RA-1 experimental reactor at a temperature similar to that used for the operation of nuclear plants (275 °C). This reactor can be used easily at different potencies. It is thus possible to keep the same spectrum at different neutron fluxes. So, it is possible to obtain the same integrated doses but at different irradiation times, i.e., different lead factors (LF). The lead factor, which is the relationship between the flux (for $E > 1$ MeV) in the specimens and the flux in the inner wall of the RPV in service, indicates the irradiation acceleration. The ASTM E 185-82 norm indicates that this factor must be greater than one and smaller than three ($1 < \mathrm{LF} < 3$). A greater LF does not guarantee that the radiation damage is similar to that suffered by the vessels in service.

The neutron spectrum in the place where the facility was located is indicated in Table 1.

Fig. 1 shows a general scheme of the irradiation facility installed in the RA1 reactor. The temperature of the Charpy V-notch specimens, the furnace power and the inert gas pressure contained in the experimental facility are controlled in the room next to the reactor.

Fig. 2 shows the device containing the eight Charpy V-notch impact specimens. The composition of the steel provided by Japan Steel Works Muroran Plant is indicated in Table 2. It complies with the probabilistic safety analysis for Atucha II-PSAR, which specifies concentrations lower than or equal to 0.10 wt.% of copper and 0.012 wt.% of phosphorus for the material of the vessel and its welds. The standard specimen ($10 \times 10 \times 55$ mm) and its orientation (T–L) are also shown in Fig. 2.

The embrittlement of the specimens after irradiation was assessed from the DBTT shift and the decrease in the upper shelf energy in impact tests on Charpy V-notch specimens. DBTT values were determined from impact testing carried out in accordance with ASTM standards.

An electron CM 200 Philips microscope was used for transmission electron microscopy (TEM) studies at an accelerating voltage of 200 kV. Specimens for TEM studies were cut from the halves of fractured Charpy specimens.

3. Irradiation plan

In most cases, the damage in the wall of the vessel is caused by a not very intense flux of fast neutrons after a long irradiation period. In an MTR, the flux is 2 to 3 – fold higher.

The neutron fast flux in the inner wall of the PHWR Atucha II reactor was estimated as $\Phi\,(E > 1\ \mathrm{MeV}) = 2 \times 10^{13}$ n m^{-2} s^{-1}. Then, for 40 years of life by design, the fluence is of about 2.5×10^{22} n m^{-2}. All the irradiations were carried out in the RA1 reactor and performed at a fluence of 6.6×10^{21} n m^{-2}, which corresponds to about 10 years of operation of the CNAII (Table 3).

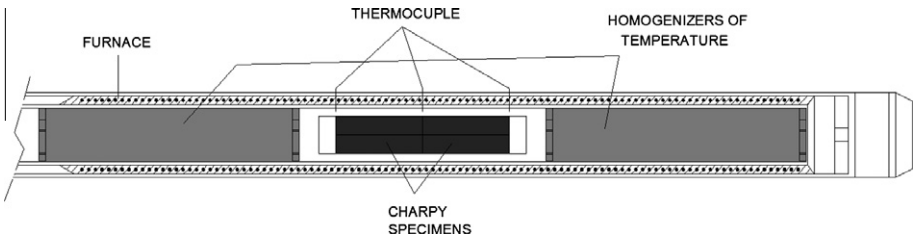

Fig. 1. Irradiation device.

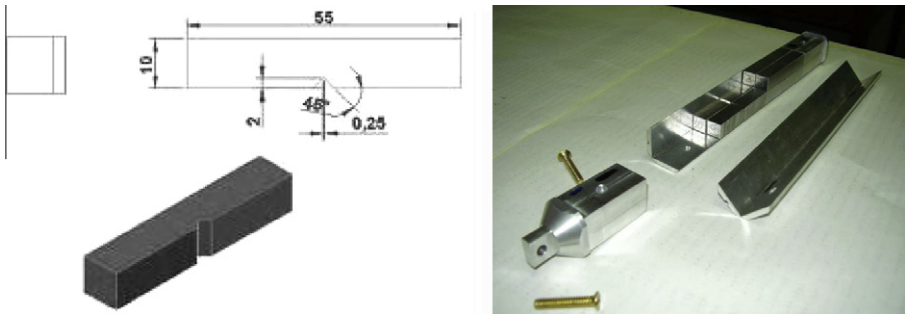

Fig. 2. Irradiation device and Charpy specimen.

Table 2
Composition of the SA-508 type 3 steel alloy (in wt.%).

C	Mn	P	S	Si	Ni	Cr	Mo	V	Cu	Al	Ta	Fe
0.25	1.40	0.012	0.015	0.15	0.74	0.2	0.53	0.03	0.1	0.05	0.03	rest

Treatment; Normalizing 920 C – 7 h, Tempering 660 C – 7 h, Quenching 885 C – 6 h 25 min, tempering 640 C – 7 h 50 min. Note: Water temperature, before quenching: 7 C, after quenching: 27 C.

Table 3
Irradiation conditions of the Charpy specimens.

	Fast flux (n m^{-2} s^{-1})	Fluence (n m^{-2})	Reactor power (kW)	Irradiation time (hours)	Lead factor
Set 1	3.715×10^{15}	6.6×10^{21}	40	492	186
Set 2	1.857×10^{15}	6.6×10^{21}	20	984	93

4. Results and discussion

The Charpy V-Notch impact specimens were tested in hot cells at various temperatures between −30 °C and 50 °C to determine the ductile-to-brittle transition behaviour. The shift of the DBTT, measured at 41 J as a measure of the brittleness of the steel, is common practice in the nuclear industry. The curves obtained from the data for the unirradiated material and the material irradiated with two lead factors are shown in Fig. 3. The curves were fitted according to the formulation of Oldfield linking the absorbed energy with the test temperature. The results of Charpy tests show shifts of the DBTT relative to the unirradiated material of $\Delta T = 14$ °C and $\Delta T = 21$ °C for irradiations with LF of 186 and 93 respectively.

There is also a significant reduction of the maximum energy absorbed. Similar decreases in the Upper Shelf Energy (USE), of the order of 100 J in ΔUSE have been documented [24–26]. In the same line, it has been long recognized that some reactor pressure vessels had materials whose USE could drop below 68 J due to neutron irradiation [27]. In these vessels, one of the actions that should be taken is a mechanics analysis of elastoplastic fracture.

A limit condition on the integrity of the pressure vessel known as pressurized thermal shock (PTS) may occur during a severe transitional system such as a loss of coolant accident (LOCA). Data of monitoring of surveillance programs establish the limit conditions for the integrity of the RPV in the case of a PTS. In such cases,

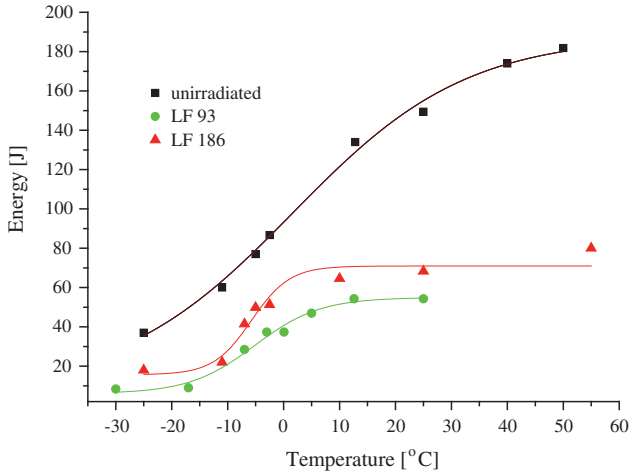

Fig. 3. Charpy curves of SA-508 type 3 steel irradiates at a fluence of 6.6×10^{21} n m^{-2}.

the limiting criterion on the embrittlement of PWR vessels, used the RT_{PTS} (nil ductility reference temperature), associated with the DBTT. Therefore, the change in the DBTT is still the parameter most used to control the degradation of materials under irradiation. However, the Charpy Test does not have with a formal basis that allows relating the DBTT to the USE unequivocally. There are models that use quantitative fractography to relate the fracture surface with the lower and upper shelf energy with the aim to know the transition temperature. For example in [28], the dispersion of the microstructure is expressed via a normal distribution of transition temperatures whereas a simple relation exists between the values of absorbed, lower and upper shelf energies, the ductile area fraction and the distribution parameters.

Transmission electron microscopy (TEM) images were obtained using a CM 200 Philips instrument. Fig. 4 shows the remarkable appearance of precipitates as a result of irradiation. The EDAX analysis indicates that these precipitates are Mn-rich precipitates.

Fig. 5 shows the TEM images for a non-irradiated sample (a), for a sample with lead factor of 93 (b) and for a sample with lead factor of 186 (c). The presence of precipitates is evident in the irradiated samples, showing an increased size for the samples with lead factor of 93. This difference is a clear sign of a nucleation and growth process during irradiation, as the samples with lead factor of 93 were irradiated for a longer time than those with lead factor of 186.

The morphology and distribution of the nanoprecipitates were analyzed with the aid of the Gatan Digital Micrograph commercial software. The results obtained for the mean diameter (D) and mean distance between them (dp) are summarized in Table 4. The corresponding histograms are shown in Fig. 6. In the case of the sample irradiated with a lead factor of 93, at a flux of 1.85×10^{15} n m^{-2} - s^{-1}, the overconcentration of vacancies above the thermodynamic equilibrium allowed the formation of precipitates with larger diameter, as shown in Fig. 6b. These precipitates showed a larger mean diameter and longer distances between each other than in the irradiation with a lead factor of 186. In the unirradiated case, almost no nanoprecipitates were. Together with the precipitates, the defects of the matrix (SMD) suggest acting similarly by blocking the advancement of dislocations depending on their size and separation distance. It is important to point that the temperature of irradiation allows only partial recovery of the agglomerates of defects created by irradiation (see Tables 5 and 6).

When the lead factor is 186, although the overconcentration of vacancies is greater, their recombination is greater, leaving fewer

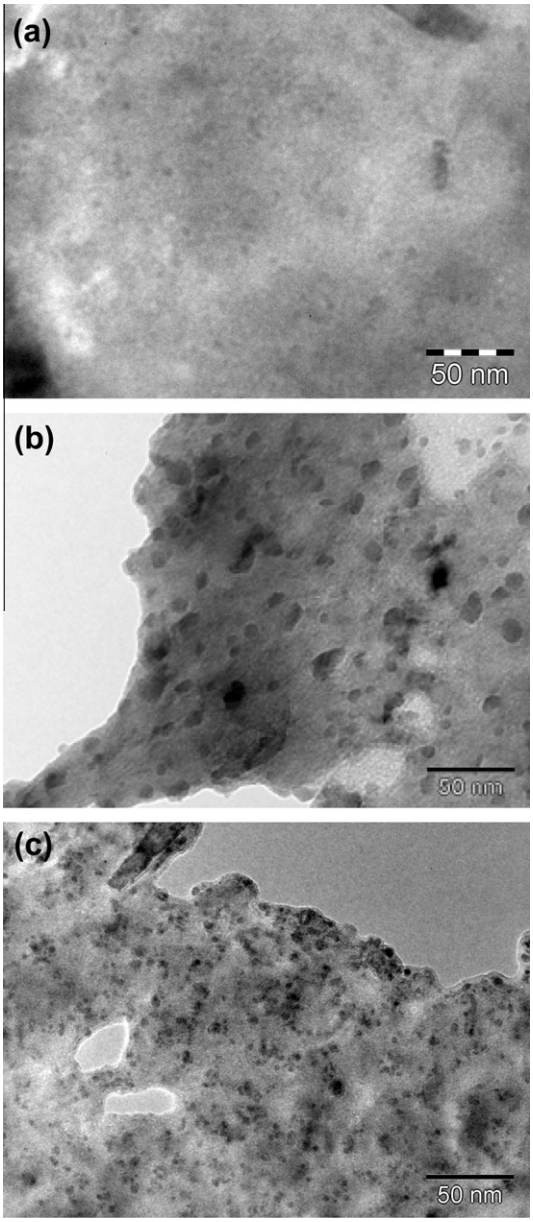

Fig. 5. Transmission electron micrographs of samples (a) unirradiated, (b) irradiated with lead factor 93 and (c) irradiated lead factor 186.

Table 4
Mean diameter (D) and average distance (dp) between precipitates.

	Lead factor	D (nm)	dp (nm)
First set	186	5 ± 1	7 ± 1
Second set	93	8.5 ± 2	25 ± 4

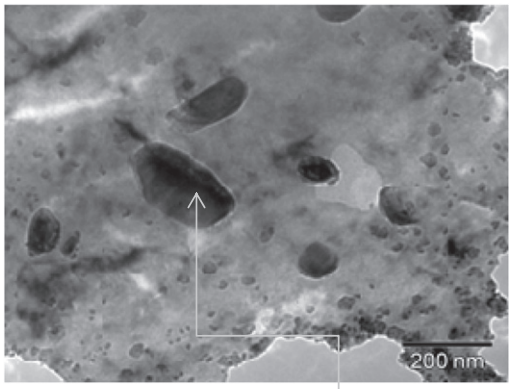

Element	Weight %	Atomic %
C K	11.9	38.7
Si K	0.3	0.4
S K	0.5	0.7
Mn K	5.1	3.6
Fe K	78.8	55
Cu K	1.5	0.9
Mo K	1.9	0.8
Total	100	100

Fig. 4. Microstructure and composition of precipitation.

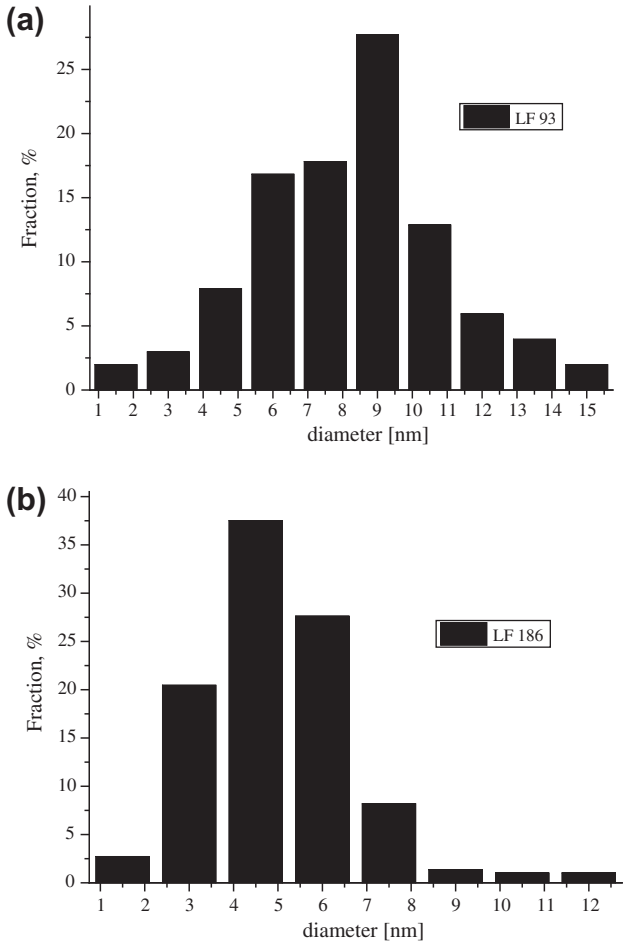

Fig. 6. Size distribution of nanoprecipitates for samples (a) irradiated with lead factor 93 and (b) irradiated lead factor 186.

Table 5
Composition determined by EDS.

Element	Weight (%)	Atomic (%)
C K	11.9	38.7
Si K	0.3	0.4
S K	0.5	0.7
Mn K	5.1	3.6
Fe K	78.8	55
Cu K	1.5	0.9
Mo K	1.9	0.8
Total	100	100

Table 6
Neutron spectrum of the inner wall Atucha II.

Neutron energy (MeV)	Neutron flux (n m^{-2} s^{-1})
0–0.1	2.99×10^{14}
0.1–1	4.81×10^{13}
1–17.33	1.93×10^{13}

vacancies for diffusion and needing a shorter time for this process. Therefore, the distribution of precipitates shows a larger number and smaller size of precipitates than in the case of a lead factor of 93, which would cause a higher blocking of the movement of dislocation (see Fig. 5c). As shown in Fig. 5c and b, the distance *dp* between precipitates is shorter for the lead factor of 186 than for the lead factor of 93. This impediment in the movement of dislocations is reflected in an increase in DBTT for a lead factor of 93. In contrast, the sample irradiated with lead factor 186 has a greater distance *dp* which facilitates the movement of dislocations. This is a mechanism similar to that of age-hardening materials [5,6].

RPV steel hardening and embrittlement result from the formation of a high number density of nanometre-size Cu–Mn–Ni precipitates and subnanometre defect cluster-solute complexes which impede dislocation glide [7]. The behaviour of precipitates and its dependence on neutron flux is explained through the kinetics of the process. For low flux levels, the concentration of thermal vacancies could be similar to the concentration of vacancies caused by irradiation. This favours the diffusion, nucleation and growth of Cu–Mn–Ni-rich precipitates [5,6].

In the case studied, the concentration of dislocations plays the role of preferential sink for point defects, which leaves fewer vacancies available for precipitation. This explains that, with a lead factor of 186 (high flux intensity and shorter irradiation time), the same fluence leads to a lower embrittlement than the irradiation corresponding to the lead factor of 93. At higher fluxes, with a lead factor of 186, the interstitial-vacancy recombination is incremented leaving less vacancies for the diffusion of alloying elements, together to the minor irradiation time. This leads to a lower embrittlement than the irradiation corresponding to the lead factor of 93.

In a predominantly thermal spectrum as the inner wall of the RPV of Atucha II, the volume of the precipitates is the structure that most contributes to the embrittlement.

The neutronic spectrum in this work has a fast component much higher than normal on the inner wall of the RPV. In a spectrum with higher proportion of fast neutrons, the great concentration of agglomerates of defects (dislocation loops) is the preferential sink for point defects, leaving fewer vacancies available for precipitation. With high lead factors, it must be considered that an intense flow of fast neutrons will not only produce defect sinks but also increase the *i*–*v* recombination, reducing the possibility of precipitation of alloying. This would account for the smaller shift of the ΔTT with regard to other fluences, without considering the differences in composition.

Taking into account the dispersion presented by Charpy tests, we advanced in the study by magnetic properties that provide macroscopic information using small amounts of irradiated materials and with greater accuracy. This work is under development; there are lines of investigation [29] that propose it as a complement for the control of the monitoring of programs in situ. Also a new irradiation was initiated with a lower lead factor.

5. Conclusions

In this paper, flux effect was examined in the low fluence regime by comparing irradiated fracture mechanical obtained on A508 Class 3 steel at the RA1 experimental reactor. The results show that the shift of the DBTT with a lead factor of 93 is larger than that obtained with a lead factor of 186. In consequence, the experimental results showed that the samples irradiated at the lower lead factor tended to have a higher embrittlement. The TEM analysis show radiation increased precipitates, mainly Cu–Ni–Mn ones. Their sizes and spacing determined the hardening and embrittlement of the steel. Then the results of irradiation in experimental reactors with high lead factors tended to be not conservative with respect to the actual RPV embrittlement.

Acknowledgments

This work was supported within the IAEA Technical Co-operation Project ARG/4/093-92 04. Project: SUPPORTING AGEING

MANAGEMENT FOR THE LONG-TERM OPERATION OF ATUCHA II NUCLEAR POWER PLANT. The authors wish to thank all operators RA1 reactor and Dr. Martin Saleta for his assistance in TEM sample preparation.

References

[1] G.E. Lucas, G.R. Odette, Advances in understanding radiation hardening and embrittlement mechanisms in pressure vessels steels, in: Proceedings of the Second International Symposium on Environmental Degradation Materials in Nuclear Power Systems-Water Reactors, ANS, Illinois, 1986, pp. 345.
[2] T. De la Rubia, V.V. Bulatov, MRS Bull. 26 (2001) 169.
[3] S. Jumel, J.C. Van Uysen, J. Ruste, C. Domain, J. Nucl. Mater. 346 (2005) 79–97.
[4] G.R. Odette, B.D. Wirth, D.J. Bacon, N.M. Ghoniem, MRS Bull. 26 (2001) 176.
[5] G.R. Odette, G.E. Lucas, Radiat. Eff. Def. Solids 144 (1998) 189–231.
[6] G.R. Odette, T. Yamamoto, D. Klingensmith, Philos. Mag. 85 (2005) 779–797.
[7] K.C. Russel, L.M. Brown, Acta Met. 20 (1972) 969.
[8] M. Caro, A. Caro, Phil. Mag. 80 (2000) 1365–1378.
[9] S.B. Fisher, J.E. Harbottle, N. Aldrige, Philos. Trans. Roy. Soc. London A 315 (1985) 301.
[10] S.B. Fisher, J.T. Buswell, Int. J. Press. Vessels Pip. 27 (1987) 91.
[11] Reactor Embrittlement Database (PR-EDB).
[12] E.D. Eason, J.E. Wright, G.R. Odette, Improved Embrittlement Correlations for Reactor Pressure Vessel Steels, NUREG/CR-6551 (Washington, DC: U.S. Government Printing Office, U.S. Nuclear Regulatory Commission, 1998).
[13] G.R. Odette, G.E. Lucas, Embrittlement of nuclear reactor pressure vessels, Light Water Reactors: Overview, JOM 53 (7) (2001) 18–22.
[14] W. Server, C. English, D. Naiman, S. Rosinski, Charpy Embrittlement Correlations Status of Combined Mechanistic and Statistical Bases for U.S. RPV Steels (MRP-45), PWR Materials Reliability Program (PWRMRP) 1000705, Final report, 2001.
[15] B.D Wirth, On the Character of Nano-Scale Features in Reactor Pressure Vessel Steels Under neutron irradiation, Ph. D. Thesis, Department of Materials, UC Santa Barbara, 1998.
[16] EPRI-CRIEPI Workshop on Dose rate Effects in RPV Materials, Olympic Valley, CA, US, November (2001) 12-14. EPRI, Palo Alto, California: 2002, and CRIEPI, Tokyo, Japan.
[17] R. Chaoudi, R. Gerard, J. Nucl. Mater. 418 (2011) 137–142.
[18] S. Jumel, J.C. Van Duysen, J. Ruste, C. Domain, J. Nucl. Mater. 346 (2005) 79–97.
[19] B.A. Gurovich, E.A. Kuleshova, O.V. Lavrenchuk, K.E. Prikhodko, Ya.I. Shtrombakh, J. Nucl. Mater. 264 (1999) 333–353.
[20] E. Mader, Kinetics of Irradiation Embrittlement and the Post Irradiation Annealing of Nuclear Reactor Pressure Vessel Steels, Ph. D. Thesis, Departament of Materials, UC Santa Barbara, 1995.
[21] G.E. Lucas, J. Nucl. Mater. 407 (2010) 59–69.
[22] P. Asoka-Kumar, B.D. Wirth, P.A. Sterne, R.H. Howell, G.R. Odette, Philos. Mag. 82 (2002) 609–615.
[23] D.E. Alexander, B.J. Kestel, P.R. Jemian, G.R. Odette, D. Klingensmith, D. Gragg, Mater. Res. Soc. Symp. Proc. 540 (1999) 415.
[24] Analysis of the behaviour of Advanced Reactor Pressure Vessel Steels under Neutron Irradiation, IAEA, VIENNA, 1986, STI/DOC/10/265.
[25] L.E. Steele, Radiation embrittlement and surveillance of nuclear reactor pressure vessels an international study, ASTM STP 819 (1981) 116.
[26] L.E. Steele, J.R. Hawthorne, Neutron embrittlement of Reactor Pressure Vessel Steels, NRL, Report 5984, 1963.
[27] V. Pontikis, D. Gorse, J. Nucl. Mater. 391 (2009) 109–113.
[28] Francis A. Pineau (Ed.), From Charpy to Present Impact Testing, Elsevier Science Ltd. and ESIS, 2002.
[29] S. Kobayashi, H. Kikuchi, S. Takahashi, Y. Kamada, K. Ara, T. Yamamoto, D. Klingensmith, G.R. Odette, J. Nucl. Mater. 384 (2009) 109–114.